Ghosh, S., Weers, J. G., Petrin, M., & Maki, A. H. (1984) *Chem. Phys. Lett. 108*, 87-93.
Ghosh, S., Zang, L.-H., & Maki, A. H. (1988) *J. Chem. Phys. 88*, 2769-2775.
Hershberger, M. V., & Maki, A. H. (1980) *J. Inorg. Biochem. 13*, 273-282.
Longworth, J. W. (1971) in *Excited States of Proteins and Nucleic Acids* (Steiner, R. F., & Weinryb, I., Eds.) pp 319-484, Plenum, New York and London.
Philips, L. A., & Levy, D. A. (1986) *J. Chem. Phys. 85*, 1327-1332.
Prabhumirash, L. S., Kutty, D. K. N., & Bhide, A. S. (1983) *Spectrochim. Acta. Part A 39A*, 663-668.
Remington, S. J., Anderson, W. F., Owen, J., Ten Eyck, L. F., Grainger, C. T., & Matthews, B. W. (1978) *J. Mol. Biol. 118*, 81-89.
Siegel, S. M. (1979) M.S. Thesis, University of California, Davis.
Steinberg, I. (1971) *Annu. Rev. Biochem. 40*, 83-114.
Turoverov, K. K., Kuznetsova, I. M., & Zaitsev, V. N. (1985) *Biophys. Chem. 23*, 79-89.
Ugurbil, K., & Bersohn, R. (1977) *Biochemistry 16*, 895-901.
Ugurbil, K., Maki, A. H., & Bersohn, R. (1977a) *Biochemistry 16*, 901-907.
Ugurbil, K., Norton, K., Allerhand, A., & Bersohn, R. (1977b) *Biochemistry 16*, 886-894.
Weber, G. (1960) *Biochem. J. 75*, 335-345.
Yamamoto, Y., & Tanaka, J. (1972) *Bull. Chem. Soc. Jpn. 45*, 1362-1366.
Zuclich, J., Schweitzer, D., & Maki, A. H. (1973) *Photochem. Photobiol. 18*, 161-168.

Comparative Triplet-State Properties of the Three Tryptophan Residues in Bacteriophage T4 Lysozyme and in the Enzyme Complex with Methylmercury(II)†

Li-Hsin Zang, Sanjib Ghosh, and August H. Maki*
Department of Chemistry, University of California, Davis, California 95616
Received May 6, 1988; Revised Manuscript Received June 17, 1988

ABSTRACT: Triplet-state energies, zero-field splittings (ZFS), and total decay rate constants of the individual triplet-state sublevels of the tryptophan (Trp) residues located at positions 126, 138, and 158 in bacteriophage T4 lysozyme have been determined by using low-temperature phosphorescence and optical detection of magnetic resonance spectroscopy in zero applied magnetic field. An investigation of spectral and kinetic properties of individual Trp residues was facilitated by measurements on point-mutated proteins containing two Trp → Tyr substitutions. We find that the phosphorescence lifetime of the buried Trp-138 is considerably shorter than those of the solvent-exposed Trp residues. CH_3Hg^{II} binding to cysteine residues in T4 lysozyme selectively perturbs the triplet state of Trp-158 by means of an external heavy-atom effect. In contrast with the previous observation of selective x-sublevel perturbation in the Trp–CH_3Hg complex, the radiative character of the z sublevel (z is the out-of-plane axis) is selectively enhanced due to the heavy-atom perturbation of Trp-158. The observed pattern of radiative and total sublevel decay constants of the perturbed Trp is attributed to a special orientation of the Hg atom with respect to the indole plane.

Bacteriophage T4 lysozyme is an interesting enzyme for studies related to protein structure and function for several reasons. It has been well characterized biochemically, and various mutated enzymes which differ from the wild-type enzyme in thermodynamic stability and in intrinsic catalytic activity have been studied (Ellwell & Schellman, 1975, 1977, 1979; Schellman et al., 1981). The crystal structures of the wild-type enzyme and of several mutants have been determined at 0.17-nm resolution (Matthews & Remington, 1974; Remington et al., 1978; Weaver & Matthews, 1987). The overall structure of the wild-type T4 lysozyme (18 700 daltons) is roughly ellipsoidal with a diameter of about 3 nm and a length of about 5 nm. It has a bilobal structure with the active site located at the conjunction of the two domains. The enzyme has 164 amino acid residues that include 3 Trp residues located at positions 126, 138, and 158 and 2 cysteine (Cys) residues at positions 54 and 97. The crystal structure (Matthews & Remington, 1974; Remington et al., 1978; Weaver & Matthews, 1987) shows that Trp-126 and -158 are at the protein surface and that Trp-138 is a buried residue located near the active site of the protein. Recently, Hudson and co-workers (Hudson et al., 1986; Harris et al., 1986) have studied T4 lysozyme and its several mutants using fluorescence anisotropy decay to probe the Trp environments as well as the perturbation of Trp environments resulting from point mutations.

Optical detection of magnetic resonance (ODMR)[1] of the triplet state is a useful technique to probe Trp and Tyr residues in proteins (Maki, 1984; Davis & Maki, 1984) and to investigate protein–nucleic acid interactions (Khamis et al., 1987) as well as protein–lipid interactions (Mao et al., 1985, 1986, 1987). Our recent investigation (Ghosh et al., 1988) of long-range nonradiative singlet–singlet energy transfer among the Trp residues in T4 lysozyme was carried out by utilizing low-temperature phosphorescence and ODMR methods. That study showed that Trp-126 transfers energy efficiently and

† This work has been supported by grants from the National Science Foundation (CHE 85-08752) and from the National Institutes of Health (ES-02662).
* Author to whom correspondence should be addressed.

[1] Abbreviations: D and E, triplet-state zero-field splitting parameters; DTT, dithiothreitol; MIDAS, molecular interactive display and simulation; MIDP, microwave-induced delayed phosphorescence; ODMR, optical detection of triplet-state magnetic resonance; ZFS, zero-field splitting(s).

0006-2960/88/0427-7820$01.50/0

selectively to Trp-158. The different energy-transfer efficiencies observed among the Trp residues were explained by noting the differing geometric orientations between Trp residues.

In this paper, we explore the environments of the Trp residues of T4 lysozyme in further detail, and we report the phosphorescence lifetimes and triplet sublevel decay rate constants of each Trp residue in the enzyme. For this purpose, several mutants containing two Trp → Tyr substitutions were studied. Furthermore, in this paper, we report on the effect of methylmercury (CH_3Hg^{II}) binding to the wild-type enzyme and to the mutants having one or two Trp → Tyr substitutions. Only Trp-158 was observed to undergo a heavy-atom perturbation as a result of CH_3Hg^{II} binding to the nearby cysteine-97. We present the phosphorescence, the lifetime, and triplet-state sublevel kinetics of Trp-158 in the CH_3Hg^{II} complexes with the wild-type enzyme and with the single Trp-158-containing mutant. The sublevel kinetics of the complexes are compared with those of the Trp–CH_3Hg^{II} complex studied previously (Anderson & Maki, 1980; Svejda et al., 1978). The selective enhancement of the radiative character of the z sublevel (where z is the out-of-plane axis of the indole ring) is interpreted in terms of a special orientation of Hg with respect to Trp-158 resulting from a suggested local conformational change upon complex formation.

Materials and Methods

Samples of bacteriophage T4 lysozyme and of the different mutants were generous gifts from L. McIntosh, Institute of Molecular Biology, Eugene, OR. The proteins were stored in 100 mM sodium phosphate buffer containing 500 mM NaCl and 0.01% NaN_3, pH 6.5–6.8. To achieve simplicity in nomenclature of the wild-type and mutated enzymes, we represent residues 126, 138, and 158 by a three-letter triplet. Thus, for example, WWW represents the wild-type enzyme, while the single-point mutant used in this work, WWY, stands for Trp-126, Trp-138, and Tyr-158. The three double-point mutants studied are WYY, YWY, and YYW.

In order to prevent the oxidation of cysteine residues, dithiothreitol (DTT) was added to each stock solution. For low-temperature spectroscopic measurement, the protein solution was mixed with 30% glycerol (Aldrich, Gold label) by volume.

Before heavy-atom modification, DTT was removed from the protein solution by exchanging the buffer solution. Methylmercury iodide (12 mM solution in ethylene glycol) was then added to the freshly prepared protein solution to produce a 4:1 molar ratio of CH_3Hg^{II} to protein. Subsequently, glycerol was added to produce a 30% by volume solution for spectroscopic measurements.

The low-temperature phosphorescence and ODMR equipment has been described previously (Ghosh et al., 1984).

ZFS was determined by ODMR slow-passage measurements in which resonances are detected by monitoring the phosphorescence intensity change upon sweeping the microwaves slowly through the transition between two sublevels. The average decay constant of Trp was obtained from phosphorescence decay measurement at 77 K. The total decay constants of the triplet-state sublevels for each Trp were measured by the microwave-induced delayed phosphorescence (MIDP) technique (Schmidt et al., 1971) and by the microwave-saturated decay technique (Zuclich et al., 1974). The relative radiative decay rates of the triplet sublevels were determined by ODMR fast-passage experiments in which the microwaves are swept through a transition pair more rapidly than the shorter lived sublevel decay time in the transition pair

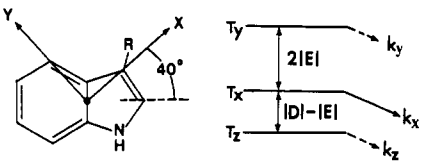

FIGURE 1: Principal axes convention and triplet-state sublevel splittings of tryptophan in zero field. Dashed arrows originate from sublevels normally decaying radiationlessly.

(Winscom & Maki, 1971). All decay data were deconvoluted by a nonlinear least-squares Marquardt algorithm designed to minimize the χ^2 of the fitting function and whose goodness-of-fit was monitored by a residuals plot. The kinetic models assumed for the MIDP, ODMR fast-passage, and the microwave-saturated phosphorescence decay measurements are given in the appropriate references cited above. As far as the phosphorescence decay measurements are concerned, the data at 77 K were fit with good agreement to two exponential components. We assumed that the major long-lived component of the decay was due to the Trp triplet state. The minor (<20%) shorter lived decay constant was similar to that observed when monitoring the emission to the blue of Trp, and was assigned to the Tyr triplet state.

The conformational study of CH_3Hg^{II} complexes was facilitated by using the molecular interactive display and simulation (MIDAS) system which is a computer software developed by the Computer Graphics Laboratory at the University of California, San Francisco. The crystal structure data of L. Weaver and B. Matthews for T4 lysozyme available in the Protein Data Bank were used for the study. Attachment of the CH_3Hg group to cysteine-97 was done by using the "addgrp" program in MIDAS; in this application, we set the S–Hg bond length to 2.1 Å, the Hg–C(Me) bond length to 1.9 Å, the C_β–S_γ–Hg bond angle to 104°, and the S_γ–Hg–C(Me) bond angle to 180°. Simulation of the local conformational change was done by using the "rotation" program to rotate Trp-158 and CH_3Hg^{II} attached to cysteine-97 about the C_α–C_β and C_β–S_γ bonds, respectively.

Results and Discussion

Phosphorescence Spectra. The phosphorescence spectra of WWW and the mutants containing a single Trp residue (WYY, YWY, and YYW) at 4.2 K have been discussed previously (Ghosh et al., 1988). It was observed that the triplet-state energies of the three Trp residues are $E_T(126) > E_T(158) > E_T(138)$ (Table I). WWW exhibits two distinct phosphorescence 0,0 bands at 407.8 and 413.6 nm corresponding to Trp-158 and Trp-138, respectively (Table I). Studies of the phosphorescence of WWY, WYW, and YWW indicated that the quenching of Trp-126 in WWW is due to efficient singlet-singlet nonradiative energy transfer from Trp-126 to Trp-158. The fraction of singlet energy transferred was found to be 0.26 for the Trp-126–Trp-158 pair, 0.05 for the Trp-126–Trp-138 pair, and undetectable for the Trp-126–Trp-138 pair. This selective efficiency of energy transfer between Trp-126 and Trp-158 was explained by their favorable orientation factor of the Förster equation and the assumption that the transition moment direction lies along the x axis in Trp (Ghosh et al., 1988) (Figure 1).

The phosphorescence spectra of the complexes of CH_3Hg^{II} with WWW, YYW, and WWY are presented in Figure 2. The complexes with WWW and YYW exhibit very intense, similar phosphorescence spectra with the 0,0 band peaking at 410.1 nm (Table I). The mutant WWY, however, when treated with CH_3Hg^{II} under the same conditions, shows the same phosphorescence spectrum as that of the uncomplexed

Table I: Phosphorescence 0,0 Band Wavelength and ZFS Parameters of the Lowest Triplet State of the Trp Residues in Bacteriophage T4 Lysozyme and Its Complex with CH_3Hg^{II}

system	$\lambda(0,0)^a$ (nm)	$\lvert D\rvert - \lvert E\rvert^b$ (GHz)	$2\lvert E\rvert^b$ (GHz)	$\lvert D\rvert + \lvert E\rvert^b$ (GHz)	$\lvert D\rvert$ (GHz)	$\lvert E\rvert$ (GHz)
WWW	407.8	1.78	2.47		3.01	1.24
	413.6	1.63	2.70		2.97	1.35
WYY	404.6	1.79 (60)	2.46 (140)		3.02	1.23
YYW	408.1	1.79 (70)	2.47 (140)		3.02	1.24
YWY	413.5	1.63 (40)	2.69 (50)		2.97	1.34
WWY	404.6	1.79	2.46		3.02	1.23
	413.4	1.63	2.68		2.97	1.34
WWW-CH_3Hg^{II}	410.1	1.74	2.5 (vw)	4.09	2.91[c]	1.18[c]
YYW-CH_3Hg^{II}	410.1	1.73		4.08	2.90[c]	1.18[c]
WWY-CH_3Hg^{II}	404.8	1.80	2.46		3.03	1.23
	413.7	1.64	2.68		2.98	1.34

[a] Peak wavelength of the 0,0 band measured at 4.2 K, with ±0.2-nm accuracy. [b] Measured at 1.2 K monitoring the 0,0 band peak. Corrected full width of the transition at half-maximum in megahertz appears in parentheses. vw = very weak. [c] Calculated by using the $\lvert D\rvert - \lvert E\rvert$ and $\lvert D\rvert + \lvert E\rvert$ transitions corresponding to the perturbed Trp-158.

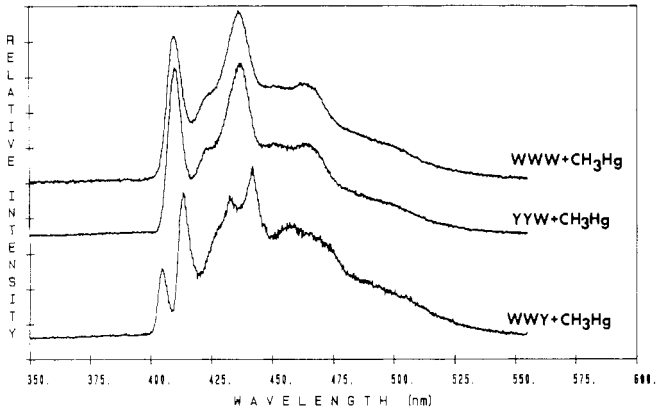

FIGURE 2: Phosphorescence spectra of the CH_3Hg^{II} complexes of WWW, YYW, and WWY in phosphate buffer containing 30% glycerol at 4.2 K with emission monochromator resolution of 1.5 nm. Excitation wavelength is 295 nm. The concentration of the enzyme in each sample is ca. 1×10^{-4} M. The molar ratio of the enzyme to CH_3Hg^{II} is 1:4 in the complexes.

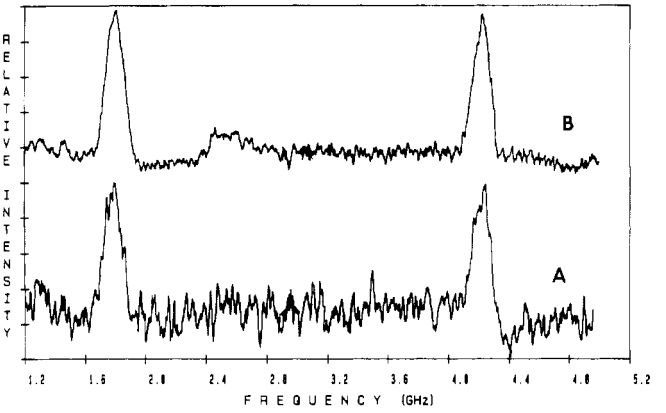

FIGURE 3: Slow-passage ODMR transitions at 1.2 K monitoring the 0,0 band of (A) the CH_3Hg^{II} complex of YYW and (B) the CH_3Hg^{II} complex of WWW. The sweep rate was 2 GHz/s, and the emission bandwidth was 1.5 nm.

WWY (Ghosh et al., 1988) (Table I). Comparison of the spectra indicates that only Trp-158 is perturbed by CH_3Hg^{II} binding to cysteine residues. The enhancement of Trp-158 phosphorescence in the CH_3Hg^{II} complexes of WWW and YYW results from the external heavy-atom effect induced by Hg attached to the nearby Cys-97, which enhances the spin–orbit coupling between singlet and triplet states. The 0,0 band of the perturbed Trp 158 is red-shifted by 2 nm relative to that of the unperturbed residue at 4.2 K (Table I). The disappearance of the 0,0 band of Trp-138 in the WWW complex probably is due to the considerable increase in the intensity of Trp-158 phosphorescence, its red-shift, and/or energy-transfer quenching.

ODMR Transitions and Zero-Field Splitting (ZFS). The slow-passage ODMR experiments monitoring the 0,0 band of the Trp residue in WYY, YWY, and YYW at 1.2 K show that all Trp residues exhibit two transitions, viz., $2|E|$ (the transition between x and y sublevels) and $|D| - |E|$ (the transition between x and z sublevels) (Table I, Figure 1). Trp-126 and -158 have similar ZFS, while the D and E values of Trp-138 are lower and higher, respectively, than those of Trp-126 and -158. The broader transition line width observed in Trp-126 and -158 relative to Trp-138 is consistent with the crystal structure in that these two residues are more solvent exposed than Trp-138. The narrow line width found for Trp-138 is indicative of a buried residue in a relatively homogeneous environment (Maki, 1984; Davis & Maki, 1984).

The slow-passage ODMR transitions monitoring the 0,0 bands of the CH_3Hg^{II} complexes of WWW and YYW at 1.2 K are presented in Table I and Figure 3. The symmetrical nature of the signals, which lack rapid-passage effects, demonstrates that the ODMR signals originate from a perturbed Trp residue having short sublevel lifetimes. In the CH_3Hg^{II}-complexed WWY, Trp-126 and -138, which are not perturbed by CH_3Hg^{II} binding, show similar $|D| - |E|$ and $2|E|$ transition frequencies as those found in the case of WWY (Table I). No $|D| + |E|$ signal is observed, which is normally the case for Trp in the absence of a heavy-atom perturbation. On the other hand, the CH_3Hg^{II}-complexed WWW exhibits very strong $|D| - |E|$ and $|D| + |E|$ signals while the $2|E|$ signal is observed with only very weak intensity. Similarly, Trp-158 in CH_3Hg^{II}-complexed YYW gives very strong $|D| - |E|$ and $|D| + |E|$ signals while the $2|E|$ signal is not detectable. The appearance of the $|D| + |E|$ signal, which is absent in normal Trp, provides convincing evidence of the external heavy-atom effect which alters the radiative character of triplet-state sublevels of Trp-158. The disappearance of the $2|E|$ transition of Trp-158 could be due to the possibility either that the z sublevel is the only radiative sublevel or that the x and y sublevels have equal steady-state populations, or to both. The triplet sublevel depopulating rates determined by transient microwave experiments discussed in a later section provide information on the radiative character of the perturbed triplet-state sublevels of Trp-158.

The D and E values obtained for the perturbed Trp-158 each are less than the values observed for any unperturbed Trp residues in this enzyme (Table I).

The wavelength-selected ODMR measurements for Trp-126, -138, and -158 in T4 lysozyme were described in an earlier paper (Ghosh et al., 1988). Since the ODMR signals of

Table II: Triplet Sublevel Total Decay Constants for Trp Residues in T4 Lysozyme

system[a]	λ(0,0) (nm) monitored	k_x (s^{-1})	k_y (s^{-1})	k_z (s^{-1})	k^*_{av}[c] (s^{-1})	k_{av} (s^{-1}) at 77 K
WYY	404.6	0.27	0.15[b]	0.06	0.157	0.163
YYW	408.1	0.24	0.12[b]	0.07	0.143	0.145
YWY	413.5	0.39	0.11	0.06	0.203	0.200

[a] Measurements were made at 1.2 K by the MIDP method. [b] Calculated from $\sum k_i = 3k_{av}$. [c] k^*_{av} is measured at 1.2 K by saturating the $|D| - |E|$ and $2|E|$ transitions simultaneously during the decay.

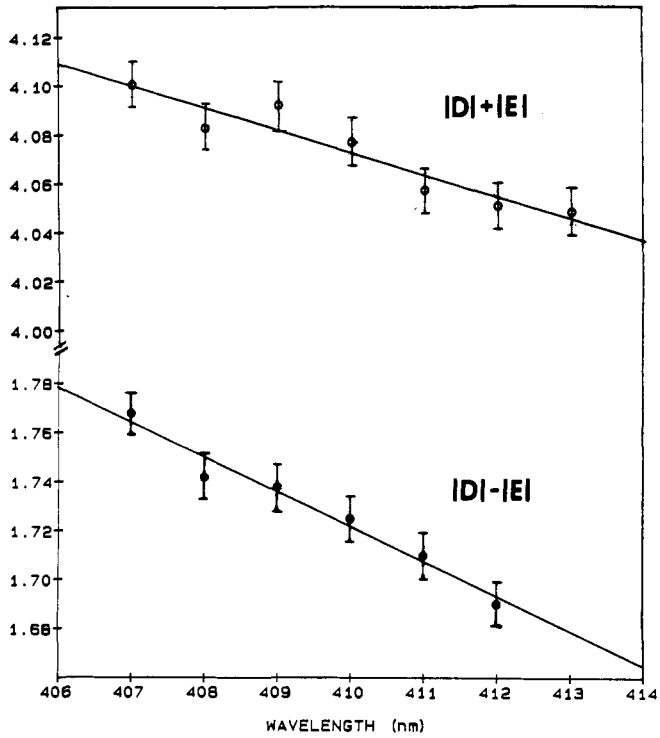

FIGURE 4: Plot of the $|D| - |E|$ and $|D| + |E|$ ODMR transition frequency vs emission wavelength monitored through the 0,0 band region of the CH_3Hg^{II} complex of YYW. The microwave sweep rate was 2 GHz/s. The temperature was 1.2 K, and the emission bandwidth was 1 nm. The transition frequencies were corrected for rapid-passage effects. The frequency error is estimated to be ±10 MHz.

Trp-158 in YYW are weak, it is difficult to make any definite conclusion regarding the wavelength dependence of the ZFS. Wavelength-selected ODMR measurements for both the $|D| - |E|$ and $|D| + |E|$ transitions of the heavy-atom-perturbed Trp-158 in the complexed YYW have been carried out. The results are plotted for the transition frequency vs monitored wavelength (Figure 4). It is clear that ZFS varies linearly with the wavelength monitored across the 0,0 band of the perturbed Trp. The wavelength dependence of the ZFS in this case is similar to that observed previously for Trp-126 in WYY (Ghosh et al., 1988), a residue known to be solvent exposed (Matthews & Remington, 1974; Remington et al., 1978; Weaver & Matthews, 1987).

Triplet-State Lifetime and Sublevel Decay Constants. The triplet-state sublevel kinetics were measured for each Trp residue by studying the single Trp-containing mutants. The average lifetime of the lowest triplet state of the individual Trp residue in WYY, YWY, and YYW at 77 K, where thermally activated spin–lattice relaxation equalizes the three sublevel populations, was measured by monitoring the 0,0 band; the results are listed in Table II. The lifetime of Trp-138 is significantly shorter than those of Trp-126 and -158.

The decay constants of the nonradiative sublevel for each Trp residue were measured by the MIDP technique (Schmidt et al., 1971) and are given in Table II. The triplet-state decay constants measured at 77 K also have been compared with the average decay constants at 1.2 K obtained by monitoring the decay during microwave double saturation. The results, given in Table II, are in excellent agreement. Although the sublevel decay constants k_y and k_z are similar for all three Trp residues, k_x of Trp-138 is about 50% greater than the values observed for the others and accounts for the reduced triplet lifetime of Trp-138. The larger decay constant for the x sublevel observed for Trp-138 may be connected with its location in a hydrophobic environment which includes several aromatic residues. On the basis of the crystal structure, residues 137–141 in T4 lysozyme form a short helical segment which connects two longer helices (Matthews & Remington, 1974; Remington et al., 1978; Weaver & Matthews 1987).

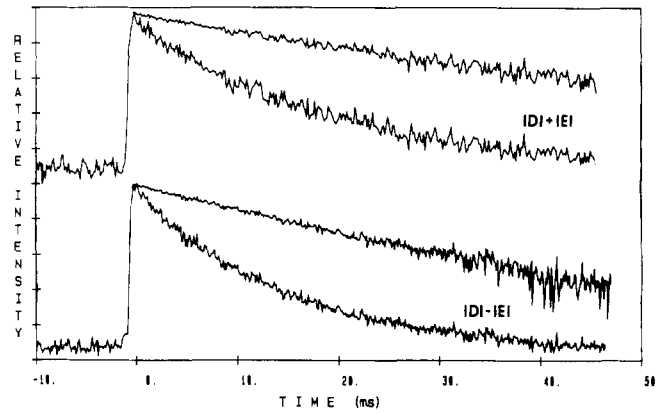

FIGURE 5: Fast-passage responses at 1.2 K of the $|D| + |E|$ and $|D| - |E|$ transitions monitoring the 0,0 band of the CH_3Hg^{II} complex of YYW. The emission bandwidth was 1 nm. The microwave sweep rate was 518 GHz/s for the $|D| - |E|$ transition and 400 GHz/s for the $|D| + |E|$ transition. The signals resulted from 5000 and 3000 scans, respectively, for the $|D| - |E|$ and $|D| + |E|$ transitions. The upper curve in each case is the logarithmic plot of the lower curve.

WWW and YYW complexed with CH_3Hg^{II} exhibit a very short lifetime (33 ms) at 77 K. This significant lifetime reduction indicates that the Trp residue is strongly perturbed by Hg which must be located at a short distance. In order to determine the relative radiative character of the triplet-state sublevels of the perturbed Trp, the microwave rapid-passage measurements for both the $|D| - |E|$ and $|D| + |E|$ transitions have been carried out by monitoring the 0,0 band of the phosphorescence at 1.2 K. The lower curves in Figure 5 show the response observed in YYW + CH_3Hg^{II}. An ODMR fast-passage signal may be analyzed by using the equation (Winscom & Maki, 1971):

$$I(t) = A_i \exp(-k_i t) - A_j \exp(-k_j t)$$

where k_i and k_j are the total decay constants of the two sublevels i and j, which are in resonance. The relative radiative decay constants are obtained from the ratio of the two preexponential factors, $k_i^r/k_j^r = A_i/A_j$ (Winscom & Maki, 1971). Figure 5 (upper curves) shows that the logarithmic plots of the rapid-passage responses for both $|D| - |E|$ and $|D| + |E|$ transitions are single exponentials which have the same decay constant within experimental error (Table III). The CH_3Hg^{II}-complexed WWW behaves similarly (Table III). These results definitely indicate that the z sublevel is the only significantly radiative sublevel in these complexes. This result

Table III: Total Triplet-State Sublevel Decay Constants and Relative Radiative Rate Constants of Trp and Trp Residues in Methylmercury-Complexed T4 Lysozyme at 1.2 K

system	λ_{exc} (nm)	λ_{obsd} (nm)	k_x (s^{-1})	k_y (s^{-1})	k_z (s^{-1})	k_{exptl} (s^{-1})	k_{calcd} (s^{-1})	k_x^r	k_y^r	k_z^r
HTrp[a]	295	406.0	0.240	0.119	0.038	0.136	0.132	1.0	<0.1	<0.1
CH_3HgTrp[b]	290	409.2	303.0	28.5	26.4	107.0	119.0	1.0	0.08	0.08
WWW–CH_3Hg^{II}	295	410.1			74.8,[c] 84.2[d]	30.2		~0.0	~0.0	1.0
YYW–CH_3Hg^{II}	295	410.1	6.2[e]	6.9[f]	73.3,[c] 70.9[d]	30.1[g]	28.8	~0.0	~0.0	1.0

[a] From Zuclich et al. (1974). [b] From Anderson and Maki (1980). [c] Determined by microwave fast passage through the $|D| + |E|$ transition. [d] Determined by microwave fast passage through the $|D| - |E|$ transition. [e] Determined by MIDP using the $|D| - |E|$ transition. [f] Determined by MIDP using the $|D| + |E|$ transition. [g] Measured at 77 K.

is consistent with the observation that the $2|E|$ transition is not detected in the CH_3Hg^{II}-complexed YYW, since the change in phosphorescence intensity accompanying a microwave slow passage through any two triplet sublevels i and j is given by

$$\Delta I_{ij} \propto (Q_i - Q_j)(N_j^0 - N_i^0)$$

where $Q = k^r/k$ is the radiative quantum yield of the sublevel and N^0 represents the steady-state population. The very weak $2|E|$ slow-passage signal detected in CH_3Hg^{II}-complexed WWW has a frequency close to that of unperturbed Trp-126 and to either perturbed or unperturbed Trp-158 (Table I). It is also accompanied by a fast-passage transient decay, characteristic of long-lived sublevels. Therefore, the very weak $2|E|$ signal could result from Trp-126 which is not perturbed in the complex or from the heavy-atom-perturbed Trp-158. Under the conditions of sample preparation, there should be negligible unperturbed Trp-158.

The total decay constants for the x and y sublevels in the CH_3Hg^{II}-complexed YYW were determined by the MIDP technique (Table III). The k_x and k_y determined for the perturbed Trp-158 have a similar value. The average decay constant calculated from the k_i's agrees very well with the decay constant measured at 77 K (Table III).

The total decay constants and the relative radiative decay constants of the triplet-state sublevels for Hg-perturbed Trp-158 in T4 lysozyme (Table III) can be compared with those found in Trp and in the Trp–CH_3Hg^{II} complex studied previously (Anderson & Maki, 1980; Svejda et al., 1978). The extent of the heavy-atom effect is much larger in the Trp–CH_3Hg^{II} complex as evidenced by the very short lifetime observed. In order to interpret the differences observed in the sublevel radiative characteristics between the perturbed Trp-158 in T4 lysozyme (in which the z sublevel is affected) and the perturbed Trp in the Trp–CH_3Hg^{II} complex (in which the x sublevel is affected), we studied the possible orientations of the CH_3Hg^{II} perturber with respect to Trp-158 in the enzyme using the available crystal structure data of WWW and the computer graphics provided by MIDAS. Several experimental (Komada et al., 1985; Chandra et al., 1978; Clark & Tinti, 1979; Ghosh et al., 1987) and theoretical (Azumi, 1973; Weinzierl & Friedrich, 1981) studies suggest that the orientation of the heavy atom with respect to the perturbed chromophore has a definite influence on the extent of the external heavy-atom effect as well as on the specific triplet sublevels affected. In our recent study of the dependence of the triplet-state sublevel properties on the location and orientation of the external heavy atom with respect to the chromophore in naphthalene-crown ether–metal ion complexes (Ghosh et al., 1987), we observed that the out-of-plane approach of the heavy-metal ion along the center of the naphthalene induces radiative character selectively into the out-of-plane sublevel. The selectivity of the sublevel dynamics can be explained in terms of symmetry restrictions which enter the spin–orbit matrix elements via overlap integrals between the π electrons

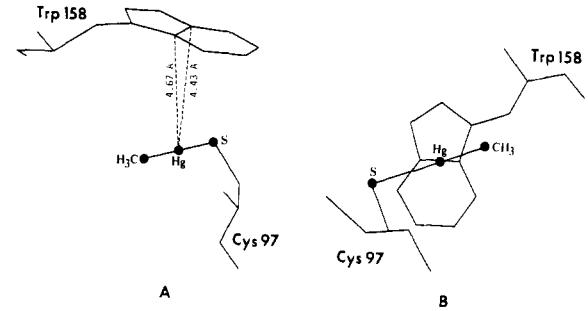

FIGURE 6: Suggested relative orientation of Trp-158 and CH_3Hg–Cys-97 obtained from a MIDAS computer study using crystal structure data of wild-type T4 lysozyme: (A) side view and (B) top view.

of naphthalene and the p orbitals of the heavy atom (Weinzierl & Friedrich, 1981; Azumi, 1973). A possible conformational change at Trp-158 upon CH_3Hg^{II} binding to Cys-97 was simulated by allowing Trp-158 to rotate around the C_α–C_β bond with a constant C_α–C_β–C_γ angle, allowing the indole ring to rotate freely around the C_β–C_γ bond, and allowing the linear CH_3HgS group to rotate simultaneously around the C_β–S_γ bond. A geometry in which the Hg atom lies close to the out-of-plane z axis of Trp-158 was obtained upon allowing the CH_3 group of CH_3Hg^{II} to become situated inside a pocket created by the conformational change. The proposed relative orientation of CH_3Hg–Cys-97 with respect to Trp-158 is shown in Figure 6. In this model, the distance between the Hg atom and the indole ring is about 4.5 Å. Although this distance is quite long for the production of a strong heavy-atom effect, the magnitude of the perturbation is maximized by the out-of-plane orientation of the perturber. In comparison with Trp–CH_3Hg, where the Hg atom is in close contact with the π system of the indole ring as suggested by NMR measurements (Svejda et al., 1978), it is not surprising that the external heavy-atom effect in the methylmercury–lysozyme system is weaker. Moreover, the selective radiative enhancement of the z sublevel of Trp-158 in CH_3Hg^{II} complexes of YYW and WWW is consistent with the computer-generated structure. The selective radiative enhancement of the x sublevel in the CH_3Hg^{II}–Trp complex suggests that the Hg atom is located close to the edge of the indole ring within the xz plane (Weinzerl & Friedrich, 1981).

In summary, triplet-state sublevel kinetic studies of the three Trp residues occurring in bacteriophage T4 lysozyme by phosphorescence and ODMR spectroscopy have been presented. The studies show that although the sublevel decay constants k_y and k_z are similar for all three Trp residues, k_x for Trp-138, which is buried, is about 50% greater than the value observed for the others, which are solvent exposed. Only Trp-158 undergoes a heavy-atom perturbation upon CH_3Hg^{II} binding to cysteine-97. The selective effect on the z sublevel is in contrast to previous results on the Trp–CH_3Hg^{II} system, in which the x sublevel is selectively perturbed. This particular sublevel selectivity observed from perturbed Trp-158 can be ascribed to the location of the Hg atom along the z axis of

Trp-158. This configuration can result from a conformational change induced by CH_3Hg^{II} binding to the surface cysteine-97. Selective enhancement of the radiative character of individual triplet sublevels can be utilized to ascertain the location of a heavy-atom perturber with respect to the local axis system of a Trp residue in additional CH_3Hg^{II}–protein systems or in complexes formed between proteins and heavy-atom-derivatized ligands.

ACKNOWLEDGMENTS

We thank L. McIntosh for his generous gift of point-mutated and wild-type T4 lysozyme samples. We also acknowledge the Computer Graphics Laboratory at the University of California, San Francisco, for the use of their computer graphics facility which made the conformational study possible.

REFERENCES

Anderson, R. R., & Maki, A. H. (1980) *J. Am. Chem. Soc. 102*, 163–167.

Azumi, T. (1973) *Chem. Phys. Lett. 19*, 580–583.

Chandra, A. K., Turro, N. J., Lyons, L. A., & Stone, P. (1978) *J. Am. Chem. Soc. 100*, 4964–4968.

Clark, S. E., & Tinti, D. S. (1979) *Chem. Phys. Lett. 60*, 292–297.

Davis, J. A., & Maki, A. H. (1984) *Biochemistry 23*, 6249–6256.

Ellwell, M., & Schellman, J. A. (1975) *Biochim. Biophys. Acta 386*, 309–323.

Ellwell, M., & Schellman, J. A. (1977) *Biochim. Biophys. Acta 494*, 367–383.

Ellwell, M., & Schellman, J. A. (1979) *Biochim. Biophys. Acta 580*, 327–338.

Ghosh, S., Weers, J. G., Petrin, M., & Maki, A. H. (1984) *Chem. Phys. Lett. 108*, 87–93.

Ghosh, S., Petrin, M., & Maki, A. H. (1987) *J. Chem. Phys. 87*, 4315–4323.

Ghosh, S., Zang, L.-H., & Maki, A. H. (1988) *J. Chem. Phys. 88*, 2769–2775.

Harris, D. L., McIntosh, L., & Hudson, B. S. (1986) *Biophys. J. 49*, 490a.

Hudson, B. S., Harris, D. L., Ludescher, R. D., Ruggiero, A., Cooney-Freed, A., & Caralier, A. S. (1986) in *Applications of Fluorescence in the Biomedical Science* (Taylor, D. L., Waggoner, A. S., Lanni, F., Murphy, R. F., & Brige, R. R., Eds.) pp 159–202, Alan R. Liss, New York.

Khamis, M. I., Casas-Finet, J. R., Maki, A. H., Murphy, J. B., & Chase, J. W. (1987) *J. Biol. Chem. 262*, 10938–10945.

Komada, V., Yamauchi, S., & Hirota, N. (1985) *J. Chem. Phys. 82*, 1651–1660.

Maki, A. H. (1984) *Biol. Magn. Reson. 6*, 187–293.

Mao, S. Y., Maki, A. H., & de Haas, G. H. (1985) *FEBS Lett. 185*, 71–75.

Mao, S. Y., Maki, A. H., & de Haas, G. H. (1986) *Biochemistry 25*, 2781–2786.

Mao, S. Y., Maki, A. H., & de Haas, G. H. (1987) *FEBS Lett. 211*, 83–88.

Matthews, B. W., & Remington, S. J. (1974) *Proc. Natl. Acad. Sci. U.S.A. 71*, 4178–4182.

Remington, S. J., Anderson, W. F., Owen, J., Ten Eyck, L. F., Grainger, C. T., & Matthews, B. W. (1978) *J. Mol. Biol. 118*, 81–98.

Schellman, J. A., Lindorfer, M., Hawkes, R., & Grutter, M. (1981) *Biopolymers 20*, 1989–1999.

Schmidt, J., Antheunis, D. A., & van der Waals, J. H. (1971) *Mol. Phys. 22*, 1–17.

Svejda, P., Maki, A. H., & Anderson, R. R. (1978) *J. Am. Chem. Soc. 100*, 7138–7145.

Weaver, L. H., & Matthews, B. W. (1987) *J. Mol. Biol. 193*, 189–199.

Weinzierl, G., & Friedrich, J. (1981) *Chem. Phys. Lett. 80*, 55–59.

Winscom, C. J., & Maki, A. H. (1971) *Chem. Phys. Lett. 12*, 264–268.

Zuclich, J., von Schütz, J. U., & Maki, A. H. (1974) *Mol. Phys. 28*, 33–47.